Computational Approach for Determination of Field-Dependent Critical Current Density for Pure MgB_2 Superconductor

Intikhab A. Ansari

Physics Division, Department of General Studies, Jubail Industrial College, P. O. Box - 10099, Jubail Industrial City-31961, Saudi Arabia

Abstract

Three empirical functions, namely linear, cubic and exponential regression functions (LRF, CRF, and ERF) are proposed in this study. The measured and predicted critical current density versus applied field, J_c (H) are evaluated for pure MgB_2 superconductors at 10, 15, and 20 K temperatures. Some statistical error estimations including Root Mean Square Error (RMSE), MABE (Mean Absolute Bias Error), and MAPE (Mean Absolute Percentage Error) reach their least values of error estimations in the exponential regression function (ERF) which reveals the most suitable function beyond its counterparts. The highest Pearson correlation coefficient, r, as well as coefficient of regression, R^2 found in ERF establish ERF as the most suitable function among all proposed functions. The study utilizes three empirical functions to determine faster and more precisely along with accurate values for computational data.

Keywords: MgB_2; Empirical functions; Critical current density; Pearson correlation coefficient

1. Introduction

The superconducting magnesium diboride, MgB_2, has received much attention in the last decade among the scientific community due to its enormous properties [1]. This material has several advantages of application such as low cost, two superconducting gaps [2], large coherence length [3], and good mechanical properties [4]. There are two important parameters of MgB_2, upper-critical magnetic field, H_{c1} and critical-current density, J_c which accomplish high values compared to conventional NbTi and Nb_3Sn [5, 6]. Therefore, MgB_2 plays an essential role in its application in various industrial areas, including current leads, energy storage devices, magnetic resonance imaging (MRI) and nuclear magnetic resonance (NMR) magnets [7–10]. On the contrary, the MgB_2 has a low irreversibility line, H_{irr}, and critical current density, J_c, has decreased as the applied magnetic field increases which shows the main disadvantage of this material [11]. Therefore, J_c is one

https://doi.org/
Published online:

of the main key elements [12] in high-temperature superconductors and the scientific community is finding a way to enhance the critical-current density, J_c by applying various techniques. The present work focuses on how the magnetic field H affects J_c in pure MgB_2 superconductors [13]. Electrical and magnetic experiments are used to determine the $J_c(H)$ dependence. The inability to establish connections in the sample and select the best voltage criterion for defining J_c reduces the consistency and reproducibility of measured values of J_c in electrical transport experiments. However, using Bean's critical state function [13] for evaluating magnetization or *ac*-susceptibility is an alternative way to determine J_c.

M. Santosh has computed the magnetic field dependency of the critical current density of the bulk MgB_2 at 20 K and modeled the critical current density of Ag-doped bulk MgB_2 [14]. In this report, he discovered an increase in critical current density with Ag content alongside a continuous decrease of magnetic field. STTE stands for superconducting transition temperature estimator which Owolabi et al. designed to directly obtain the transition temperature of the disordered MgB_2 superconductor from room temperature resistivity measurements [15]. The support regression vector (SVR) method applied by STTE achieved excellent correlation with experimental transition temperature data. M. Yazdani-Asrami et al. calculated a non-sinusoidal AC loss of superconducting tape under distorted currents using the H-formation finite element method [16]. Variations of artificial intelligence functions were applied to estimate the AC loss behavior of typical superconducting tape specimens [16]. Study of bulk MgB_2 trapped magnetic field and local critical-current distribution was conducted by Ozturk and Dancer using numerical modeling solutions [17]. The two distinct critical current models derived their basis from experimental data described in literature. [17].

The empirical functions [18] are established for rapid and accurate assessment of critical current density magnetic field dependence in pure-MgB_2 superconductors at various temperatures according to experimental data [19, 20]. The proposed functions employed statistical error estimation methods that included Root Mean Square Error (RMSE), Mean Bias Error (MBE), Mean Absolute Bias Error (MABE) and Mean Absolute Percentage Error (MAPE) [21] to determine the best empirical function by finding the minimum error [18]. J_c measurement performs smoothly through the Clem-Sanchez (CS) function irrespective of a square or circular sample shape [22].

2. Proposed modeling

The theoretical critical current density, J_c is computed using a CS function that applies to a critical-state described by the Bean function [23] in a circular disk of thickness $d \ll R_d$, where R_d is the radius of the disk. The critical-current density, J_c is the function of the characteristic field, H_d as $J_c = 2H_d/d$ [13]. The critical current density shows a steady decline as the temperature rises [24, 25],

$$\frac{J_c(T)}{J_c(0)} = \frac{H_c(T)}{H_c(0)} = \left(1-\left(\frac{T}{T_c}\right)^m\right)^n, \qquad (1)$$

where m and n are the exponents and T_c is the critical temperature of the sample [11]. One can define the effective temperature [25] with the help of the inverse function for Eq. (1).

$$\left(\frac{T}{T_c}\right)_{effective} \equiv \left(1-\left(c\frac{H_d}{H_{ac}}\right)^{1/n}\right)^{1/m}, \qquad (2)$$

where $c \equiv H_{ac} / H_d(0)$, n, m, and T_c are the fitting parameters of the CS function. As a result, the zero-temperature critical current density [13] can be defined as

$$J_c(0) = 2H_{ac}/cd \qquad (3)$$

This expression defines H_{ac} as the field amplitude along with a magnetic field dependence of critical current density, $J_c\,(T)$ which is shown in Eq (1) [24].

2.1 Proposed functions

2.1.1 Linear regression function

Linear regression function (LRF) performs variable correlation assessment by applying linear equations to analysis data points. The LRF functions by segregating one variable as the explanatory variable while designating the other variable as the dependent variable. LRF acts as both a predictor and model predictor for current data behavior patterns. The first systematic study of this regression type has become a widely used method in practical applications.

2.1.2 Cubic regression function

The cubic regression function (CRF) also known as 3rd order polynomial regression provides a better result rather than the linear regression function [18]. It is more suitable for estimating critical current, J_c as a function of the applied field, H [26]. The CRF generates an equation which matches the data points effectively and exceeds the number of data points fit by the linear plot. One can observe that RMSE has decreased, and R^2-score has increased in CRF as compared to the LRF.

2.1.3 Exponential regression function

Using an exponential regression function (ERF) means searching for an exponential function whose equation best suits the data collection. The use of an exponential regression model occurs when initial growth starts gradually and later intensifies swiftly beyond limitations. In this study, exponential regression provides the best results in comparison with linear and cubic functions.

2.2. Statistical error estimation along with functions comparison

The present research employs three proposed empirical functions which comprise LRF, CRF, and ERF [18]. These functions are analyzed and evaluated by statistical error estimation to compare the performance of these functions. In addition, the large value of r and R^2 exhibits the effectiveness of the proposed function. The following description summarizes the total sum of squares (SST) and sum of squares of regression (SSR):

Total sum of squares

$$(\mathrm{SST}) = \sum_{i=1}^{n} \left(\overline{J_{cm}} - J_{cm}{}^{i}\right)^2 \tag{4}$$

Sum of squares of regression

$$(\mathrm{SSR}) = \sum_{i=1}^{n} \left(J_{cm}{}^{i} - J_{cp}{}^{i}\right)^2 \tag{5}$$

here, J_{cm} represents the measured critical current and J_{cp} shows the predicted critical current, while $\overline{J_{cm}}$ is the mean of the measured critical current which can be described as:

$$\overline{J_{cm}} = \frac{1}{n}\sum_{i=1}^{n} J_{cm}{}^{i} \tag{6}$$

$$\text{Coefficient of Regression } (\mathrm{R}^2) = \frac{SSR}{SST} \tag{7}$$

here, SST refers to the total sum of squares while SSR defines the sum of squares of regression [18].

The Pearson correlation coefficient can be expressed as:

Correlation coefficient

$$(r) = 1 - \frac{\sum_{i=1}^{n}(J_{cm}^{i} - J_{cp}^{i})^2}{\sum_{i=1}^{n}(J_{cm}^{i} - \overline{J_{cm}})^2} \tag{8}$$

The Eqs. (7) and (8) describe the coefficient of regression (R^2) and the Pearson correlation coefficient (r), respectively, it reveals the overall performance level of the best fit across the data. The value of r close to 1 indicates the dominance of the function among the others. Both r and R^2 show high values which provide the optimal empirical function [18].

The differences between the observed and predicted responses are known as residuals. It can be thought of as the basics of variation unexplained by the fitted function. The random error values are evaluated through residuals testing. Random residuals demonstrate that the proposed function proves an accurate fit but the regular pattern shows the least accurate fit. Some statistical error estimations included in this study are RMSE, MBE, MABE, and MAPE as described below:

$$\text{RMSE} = \sqrt{\frac{1}{n}\sum_{i=1}^{n}\left(J_{cm}{}^{i} - J_{cp}{}^{i}\right)^{2}} \quad (9)$$

$$\text{MBE} = \frac{1}{n}\sum_{i=1}^{n}\left(J_{cm}{}^{i} - J_{cp}{}^{i}\right) \quad (10)$$

$$\text{MABE} = \frac{1}{n}\sum_{i=1}^{n}\left|J_{cm}{}^{i} - J_{cp}{}^{i}\right| \quad (11)$$

$$\text{MAPE} = \frac{1}{n}\sum_{i=1}^{n}\left(\left|\frac{J_{cm}{}^{i} - J_{cp}{}^{i}}{J_{cm}{}^{i}}\right| \times 100\right) \quad (12)$$

Short-term performance assessment depends on RMSE statistics while MBE provides insights into long-term evaluations. If MBE is positive, it represents over-approximation while the negative value of MBE indicates the approximation of the predicted data. The effectiveness level of a fitting function is specified by MABE [18]. The percentage error of the fitting function appears through the MAPE measure. The minimum values of RMSE, MBE, MABE and MAPE indicate the most suitable fitted empirical function [18].

3. Results and discussion

In this study, I have constructed a program for the computation of all these statistical errors and values using Python language. Fig. 1(a)–(c) illustrates the field dependency of critical current density for linear, cubic, and exponential regression functions for pristine MgB_2. The measured and predicted critical current density, J_{cm}, and J_{cp} were determined at 10, 15, and 20 K temperatures in this work. Some statistical error estimations including RMSE, MBE, MABE, and MAPE are measured by these proposed functions as shown in table 1, table 2, and table 3. The RMSE values in all three functions reveal that exponential regression demonstrates the lowest values of RMSE 4207.87, 4187.47, and 7444.95, respectively at 10, 15, 20 K temperatures, rather than other functions. In addition, MAPE has minimum values of 4.61, 3.15, and 32.67 % in the exponential regression function as compared to other functions. Notably, MABE shows the least value in ERF as 3237.77, 3291.25, and 6540.77 at a 10–20 K temperature range as compared to LRF and CRF. furthermore, the highest values of Pearson correlation coefficient, r, 0.9977, 0.9970, and 0.9985, and coefficient of regression, R^2, 0.998, 0.995, and 0.997 at 10–20K temperatures in ERF exhibit the best-fitted function amongst the other functions, LRF and CRF, as can be seen in table 3. It is remarkable from figures 1(a)–(c) that J_{cm} and J_{cp} are decreasing systematically on enhancing the temperature. Figures 1(b) and (c) represent the better $J_c(H)$ plot rather than fig. 1(a) that concludes that CRF and ERF have better dependence on data as compared to LRF [13].

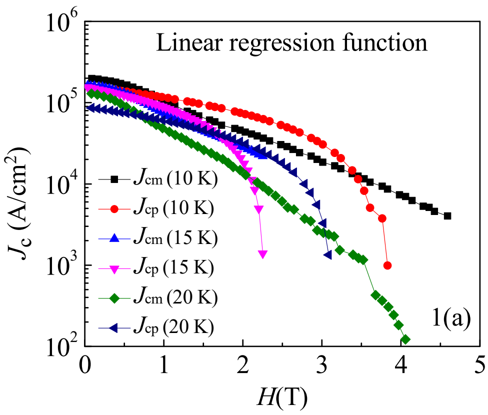

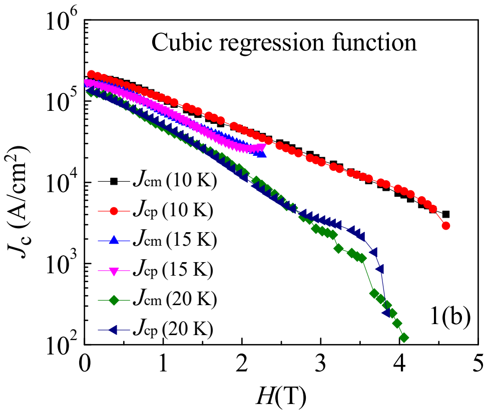

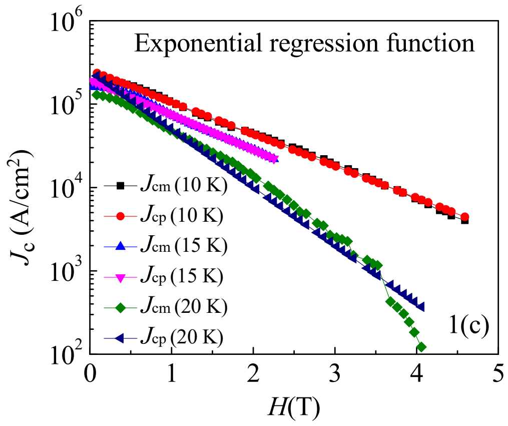

Fig 1(a)–(c): Field dependent critical current density, J_c (H) for linear, cubic and exponential regression function for pure MgB_2 sample at 10, 15, and 20 K temperature.

Fig. 2(a)–(c) demonstrates how critical current density J_c (H) varies with applied field at various temperatures 10, 15, and 20 K, individually. In all figures 2(a) to (c), The measured J_{cm} value proves consistent with the predicted J_{cp}-Exponential at all the temperatures, which shows that the ERF explicates the best-suited function among all the proposed functions. On the contrary, the curve of predicted J_{cp}-Linear has very much deviation from the measured Jcm in all the temperatures. Results used for Jcm measurements in pure MgB_2 have been obtained from my previous study [20] alongside a detailed description of the analysis method found in that report. The solid-state reaction route is used for the fabrication of MgB_2 samples [13]. All the measured and predicted J_{cm} and J_{cp} values are higher than 105 A/cm^2 in 10–20 K temperature except the J_{cp}-Linear at 20 K in fig. 2(c).

Tables 1, 2, and 3 show the linear, cubic, and exponential regression function data, respectively at 10 K, 15 K, and 20 K temperatures. Among the three tables the ERF achieved optimal r and R^2 values that almost reached 1. The MABE and MAPE values are also least in table 3 which illustrates ERF as the best-suited function at all. The second row of all the tables depicts the equation used in LRF. CRF and ERF at temperatures 10 K, 15 K, and 20 K.

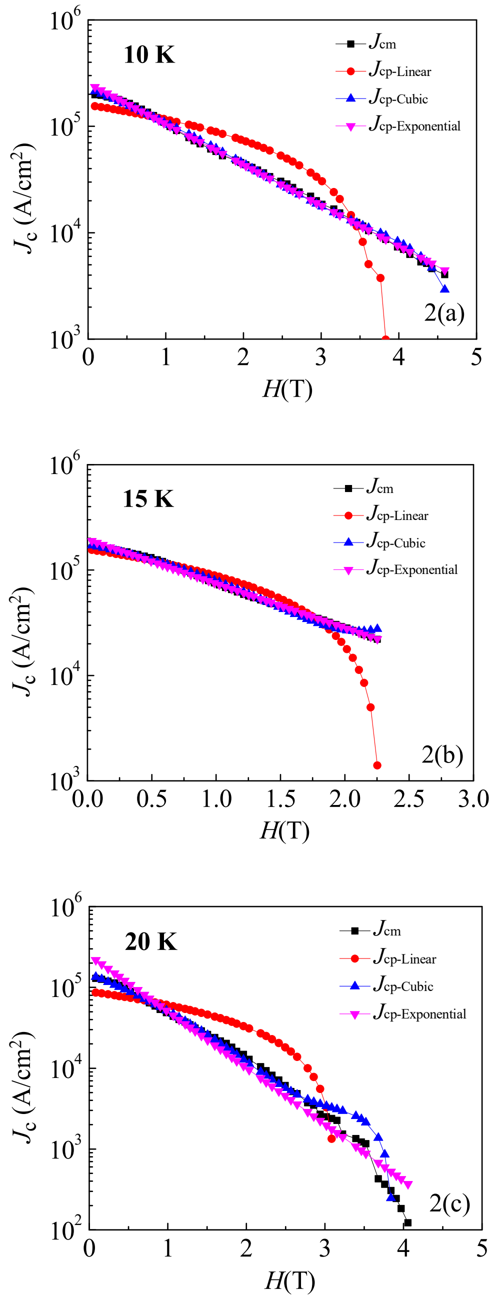

Fig 2(a)–(c): Field dependent critical current density, J_c (H) at 10, 15, 20 K temperature for pure MgB_2 sample. The linear, cubic, and exponential J_{cp}'s are compared with the measured J_{cm}.

Table 1
Linear regression function:

Empirical function	***T* = 10K**	***T* = 15K**	***T* = 20K**
Linear regression function	$J_{10K} = -42523.1\mathrm{H} + 158548.73$	$J_{15K} = -69265.021\mathrm{H} + 157459.98$	$J_{20K} = -28302.23\mathrm{H} + 88705.88$
MBE	-2550.793125	-5.99814E-07	8.00013E-07
MABE	19417.71	9526.45	15819.51
MAPE	70.01%	18.62%	1300.75%
RMSE	22793.004	10658.77	18504.88
r	0.9338	0.9731	0.8739
R^2	0.839	0.947	0.764

Table 2
Cubic regression function:

Empirical function	***T* = 10K**	***T* = 15K**	***T* = 20K**
Cubic regression function	$J_{10K} = -3165.37H^3 + 37144.98H^2 - 152500.33H + 226441.36$	$J_{15K} = -9566.92H^3 + 6861.07H^2 - 98243.47H + 174313.6$	$J_{20K} = -4373.79H^3 + 41297.49H^2 - 132016.79H + 145904.02$
MBE	-9.99829E-07	114.59	887.11
MABE	7178.45	3561.15	10661.97
MAPE	5.81%	4.48%	289.56%
RMSE	7007.67	6660.13	24069.38
r	0.9951	0.9908	0.9834
R^2	0.995	0.994	0.968

Table 3
Exponential regression function:

Empirical function	***T* = 10K**	***T* = 15K**	***T* = 20K**
Exponential regression function	$J_{10K} = 253644.97e^{-0.881H}$	$J_{15K} = 196803.847e^{-0.974H}$	$J_{20K} = 250202.76e^{-1.606H}$
MBE	-853.67	-144.48	-7953.16
MABE	3237.77	3291.25	6540.77
MAPE	4.61%	3.15 %	32.67%
RMSE	4207.87	4187.47	7444.95
r	0.9977	0.9970	0.9985
R^2	0.998	0.995	0.997

4. Conclusions

Conclusively, the field dependency of critical current density [24], $J_c(H)$ is determined for measured and predicted values of J_c at temperatures 10, 15, and 20 K for pure MgB_2 superconductor. The three empirical functions, namely linear, cubic and exponential are proposed to find the $J_c(H)$ values. Some statistical error estimation including RMSE, MABE, and MAPE shows the least values in ERF which exhibits the best-suited function better than LRF and CRF. The maximum values for Pearson correlation coefficient, r, and coefficient of regression, R^2 [18] occur closely to one at 10–20K temperatures in ERF conclude the best-fitted function among the other functions, LRF and CRF.

Acknowledgment

IAA thanks to the Chairman of Department of General Studies, Jubail Industrial College, Jubail, Saudi Arabia for the continuous support of this work.

Conflicts of Interest

The author declares no conflict of interest.

Funding

This article underwent independent research without financial support from any sources for authorship, publication, or research operations.

Data availability

The raw/processed data required to reproduce the above findings cannot be shared at this time as the data also forms part of an ongoing study.

References

[1] Zhao Q, Liu Y and Cai Qi 2013 *Materials Chemistry and Physics* **138** 192
[2] Nagamatsu J, Nakagawa N, Muranaka T, Zenitani Y, Akimitsu J 2010 *Nature* **410** 63
[3] Eisterer M, Zehetmayer M, Weber H W 2003 *Phys Rev Lett.* **90** 247002-4
[4] Murakami A, Iwamoto A, Noudem J G 2018 *IEEE Trans Appl Supercond.* **28** 8400204-4
[5] Dou S X et al. 2002 *Appl. Phys. Lett.* **81** 3419
[6] Kim J H, Zhou S, Hossain M S A, Pan A V, Dou S X 2006 *Appl. Phys. Lett.* **89** 142505
[7] Vinod K, Abhilash Kumar R G, Syamaprasad U 2007 *Supercond. Sci. Technol.* **20** R1
[8] Perini E, Ginuchi G 2009 *Supercond. Sci. Technol.* **22** 045021
[9] Muralidhar M, Inoue K, Koblischka M R, Tomita M, Murakami M 2014 *J. Alloys Comp.* **608** 102
[10] Yamamoto A, Ishihara A, Tomita M, Kishio K 2014 *Appl. Phys. Lett.* **105** 032601
[11] Chou M J, Horng H E 2010 *Annalen der Physik* **522** 128
[12] Sanchez A and Navau C 2001 *Supercond. Sci. Technol.* **14** 444
[13] 1991 *Advances in Superconductivity* III
[14] Santosh M 2016 *Acta Physica Polonica A* **129** 1197-1200
[15] Owolabi T O et al. 2016 *Applied Computational Intelligence and Soft Computing* **2016** 1-7.
[16] Asrami M Y et al. 2020 *IEEE Access* **8** 207287-207297
[17] Ozturk K and Dancer C E J 2017 *Journal of Alloys and Compounds* **693** 1109-1115
[18] Ansari I A, Rao C V 2021 *Materials Today Proceedings* **45(6)** 4417
[19] Marchi T et al. 2005 *Physica C* **426** 1264
[20] Ansari I A et al. 2013 *Physica C* **495** 208-212
[21] Ogbaka D T et al. 2021 *International Journal of Scientific Advances* **2(3)** 465
[22] Clem J R, Sanchez A 1994 *Phys. Rev. B* **50** 9355
[23] Bean C P 1964 *Rev. Mod. Phys.* **36** 31
[24] Banchewski J 2020 Ph D Thesis *Universitat Autonoma de Barcelona*
[25] Janů Z, Soukuo F 2014 *Physica C* **501** 55–61
[26] Koblischka M R et al. 2020 *AIP Advances* **10(1)** 015035